

data and for magnetic measurements. This work was supported by the Deutsche Forschungsgemeinschaft and the Fonds der Chemischen Industrie. It contains parts of a doctoral thesis by M.H.M.

Registry No. Ag₃P₁₁, 75975-89-2.

Supplementary Material Available: Listings of structure factor amplitudes and anisotropic thermal parameters of the Ag atoms (11 pages). Ordering information is given on any current masthead page.

Contribution from the Department of Chemistry,
Wayne State University, Detroit, Michigan 48202

Comparison between d¹-d¹ and d⁹-d⁹ Magnetic Exchange in Binuclear Vanadyl and Copper(II) 1,3,5-Triketonates. Crystal and Molecular Structure of Cu₂(DANA)₂(py)₂

MARY JANE HEEG, J. L. MACK, M. D. GLICK,* and R. L. LINTVEDT*

Received May 23, 1980

The binuclear complex bis(1,5-bis(*p*-methoxyphenyl)-1,3,5-pentanetrionato)bis(pyridine)dicopper(II), Cu₂(DANA)₂(py)₂, has been crystallized and examined by X-ray diffraction techniques. The structure consists of binuclear monomers in which each copper atom is bound to four ketonic oxygen atoms and an axial pyridine. Crystal data is as follows: *P*2₁/*c*, *a* = 8.413 (2) Å, *b* = 22.791 (5) Å, *c* = 11.109 (2) Å, β = 91.60 (2)°, *Z* = 2, *R*₁ = 0.035, *R*₂ = 0.050. The d⁹-d⁹ system, Cu₂(DANA)₂(py)₂, exhibits strong intramolecular antiferromagnetism ($-2J = 825 \text{ cm}^{-1}$) resulting in nearly diamagnetic behavior at room temperature. These results are contrasted to the structurally related d¹-d¹ system, (VO)₂(DANA)₂, in which the value of $-2J$ is 160 cm⁻¹. The magnetic differences are discussed in terms of the orbital symmetry of the exchanging electrons.

Introduction

An intriguing feature of the 1,3,5-triketones as a class of ligands is their ability to bind two metal ions in a relatively constant ligand environment.¹⁻⁸ In addition, in all cases studied to date in which the individual metal ions are paramagnetic, the binuclear molecules exhibit a net antiferromagnetism due to superexchange interactions. The nature of the superexchange interactions is presumably determined by the bonding interactions taking place between the metal ions and the two triketonate moieties which invariably exist in a very nearly coplanar arrangement in these complexes. Since bond lengths and angles in the parts of the molecules associated with the metal ions are found to be very similar for a variety of metal ions, differences in magnetic properties should be largely attributable to differences in the symmetry of the metal orbitals containing unpaired electrons. Hence, by investigating the magnetic properties and structures of a series of binuclear 1,3,5-triketones, it should be possible to make definitive statements about how magnetic exchange is influenced by the orbital symmetry of exchanging electrons. Perhaps the simplest comparison to be made in this regard is a d¹-d¹ system to a d⁹-d⁹ system since both contain the same number of unpaired electrons and there are no significant complications due to spin-orbit contributions. This study was undertaken

to compare the magnetic properties of structurally similar binuclear VO²⁺ and Cu(II) complexes containing the same 1,3,5-triketone ligand.

Experimental Section

Ligand Synthesis. The ligand 1,5-bis(*p*-methoxyphenyl)-1,3,5-pentanetrione, H₂DANA,⁹ was prepared by the method of Miles, Harris, and Hauser.¹⁰

Bis(1,5-bis(*p*-methoxyphenyl)-1,3,5-pentanetrionato)dioxovanadium(IV), (VO)₂(DANA)₂. A solution of 0.79 g (0.005 mol) of VCl₃ to 100 mL of absolute ethanol was prepared by refluxing and stirring. To this was added a solution of 1.6 g (0.005 mol) of H₂DANA dissolved in 100 mL of absolute ethanol followed by 0.23 g (0.01 mol) of Na metal dissolved in 50 mL of absolute ethanol. The solution was refluxed for 18 h and filtered to separate NaCl. The filtrate was concentrated under reduced pressure to 50 mL and cooled at -10 °C for 24 h. The resulting red powder melts with decomposition at 330-335 °C. Anal. Calcd for C₃₈H₃₂O₁₂V₂: C, 58.31; H, 4.09; V, 13.04. Found: C, 58.49; H, 4.59; V, 12.40.

Bis(1,5-bis(*p*-methoxyphenyl)-1,3,5-pentanetrionato)dicopper(II), Cu₂(DANA)₂. A solution of 1.0 g (0.005 mol) of Cu(C₂H₃O₂)₂·H₂O in 50 mL of methanol was heated, and a solution of 1.6 g (0.005 mol) of H₂DANA in 25 mL of CHCl₃ was added dropwise. A green precipitate formed immediately. It does not melt to 300 °C. Anal. Calcd for C₃₈H₃₂O₁₀Cu₂: C, 58.76; H, 4.12. Found: C, 58.65; H, 4.25.

Cu₂(DANA)₂(py)₂. The green Cu₂(DANA)₂ was dissolved in a small amount of pyridine. The solution was evaporated to dryness in an efficient hood to yield dark blue-green crystals of Cu₂(DANA)₂(py)₂. This product was redissolved in a minimum of pyridine which was concentrated at room temperature to about 50% of the original volume. Large dark blue crystals, suitable for single-crystal X-ray structure determination resulted. Anal. Calcd for C₃₈H₃₂O₁₀Cu₂(C₅H₅N)₂: C, 61.67; H, 4.50; N, 3.00. Found: C, 61.75; H, 4.61; N, 2.96.

Magnetic Susceptibility. Magnetic susceptibility as a function of temperature was measured with use of the standard Faraday technique

- (1) Lintvedt, R. L.; Glick, M. D.; Tomlonovic, B. K.; Gavel, D. P. *Inorg. Chem.* **1976**, *15*, 1646.
- (2) Glick, M. D.; Lintvedt, R. L.; Gavel, D. P.; Tomlonovic, B. K. *Inorg. Chem.* **1976**, *15*, 1654.
- (3) Kuszej, J. M.; Tomlonovic, B. K.; Murtha, D. P.; Lintvedt, R. L.; Glick, M. D. *Inorg. Chem.* **1973**, *12*, 1297.
- (4) Lintvedt, R. L.; Borer, L. L.; Murtha, D. P.; Kuszej, J. M.; Glick, M. D. *Inorg. Chem.* **1973**, *13*, 18.
- (5) Glick, M. D.; Lintvedt, R. L.; Anderson, T. J.; Mack, J. L. *Inorg. Chem.* **1976**, *15*, 2258.
- (6) Lintvedt, R. L.; Glick, M. D.; Tomlonovic, B. K.; Gavel, D. P.; Kuszej, J. M. *Inorg. Chem.* **1976**, *15*, 1633.
- (7) Blake, A. B.; Fraser, L. R. *J. Chem. Soc., Dalton Trans.* **1974**, 2554.
- (8) Guthrie, J. W.; Glick, M. D.; Lintvedt, R. L. submitted for publication *Inorg. Chem.*

- (9) The abbreviation H₂DANA refers to the trivial name dianisoylacetone.
- (10) Miles, M. L.; Harris, T. M.; Hauser, C. R. *J. Org. Chem.* **1965**, *30*, 1007.

Table I. Fractional Atomic Positional Parameters^a

atom	x	y	z
Cu	0.03179 (4)	0.01026 (2)	-0.13214 (3)
O(1)	0.01687 (24)	-0.05275 (9)	-0.01266 (17)
O(2)	0.10687 (25)	-0.04238 (8)	-0.24918 (18)
O(3)	0.10901 (26)	0.07854 (9)	-0.21099 (18)
C(1)	-0.00673 (35)	-0.10903 (13)	-0.03682 (27)
C(2)	0.03062 (40)	-0.13084 (14)	-0.15208 (26)
C(3)	0.08650 (35)	-0.09891 (13)	-0.24738 (27)
C(4)	0.12056 (34)	0.13000 (13)	-0.16536 (25)
C(5)	0.07062 (42)	0.14549 (14)	-0.05086 (29)
C(31)	0.12575 (36)	-0.12840 (13)	-0.36233 (26)
C(32)	0.14281 (48)	-0.18880 (14)	-0.37408 (31)
C(33)	0.18549 (54)	-0.21372 (15)	-0.48159 (33)
C(34)	0.21433 (41)	-0.17926 (14)	-0.58093 (28)
C(35)	0.19336 (48)	-0.11919 (15)	-0.57216 (30)
C(36)	0.15114 (45)	-0.09506 (15)	-0.46425 (29)
O(37)	0.25993 (34)	-0.20803 (10)	-0.68040 (20)
C(38)	0.32290 (56)	-0.17404 (21)	-0.77547 (33)
C(41)	0.19957 (36)	0.17429 (13)	-0.24124 (26)
C(42)	0.25645 (43)	0.15760 (15)	-0.35362 (29)
C(43)	0.34004 (48)	0.19612 (16)	-0.42431 (30)
C(44)	0.36902 (40)	0.25307 (14)	-0.38483 (28)
C(45)	0.30969 (46)	0.27115 (15)	-0.27591 (33)
C(46)	0.22711 (46)	0.23201 (14)	-0.20565 (30)
O(47)	0.45478 (32)	0.28760 (10)	-0.45889 (22)
C(48)	0.49999 (70)	0.34417 (21)	-0.41474 (52)
N(1)	-0.22725 (32)	-0.00075 (12)	-0.19945 (25)
C(91)	-0.34757 (56)	0.02221 (18)	-0.13890 (38)
C(92)	-0.50298 (51)	0.01982 (25)	-0.17926 (53)
C(93)	-0.53742 (55)	-0.00732 (26)	-0.28587 (56)
C(94)	-0.41605 (58)	-0.03173 (23)	-0.34955 (43)
C(95)	-0.26374 (47)	-0.02721 (18)	-0.30424 (35)

^a The esd's are given in parentheses.

with Hg[Co(SCN)₄] as the calibrant. Temperatures were measured to ±1 K. Measurements were made at field strengths of about 8000 G. Diamagnetic corrections were made with use of Pascal's constants.

Structure Determination. Precession photographs (Mo K α radiation) of the title complex indicated a monoclinic unit cell with systematic absences consistent with the space group¹¹ $P2_1/c$ ($h0l$, $l = \text{odd}$ and $0k0$, $k = \text{odd}$ absent). A crystal of approximate dimensions $0.38 \times 0.34 \times 0.80$ mm was mounted with the glass fiber coincident with the long dimension (c^*) and optically centered on a Syntex P₂ automated diffractometer. The lattice parameters previously determined from precession methods were refined by least-squares analysis of 15 precisely centered reflections ($a = 8.413$ (2) Å, $b = 22.791$ (5) Å, $c = 11.109$ (2) Å, $\beta = 91.60$ (2)°, $V = 2129.2$ (9) Å³. With two molecules per unit cell, the calculated density is 1.46 g cm⁻³.

Intensity data were collected at ambient temperatures with use of Mo K α radiation (0.71069 Å) with a graphite monochromator. A θ - 2θ scan from 1.0° below $K\alpha_1$ to 1.0° above $K\alpha_2$ was used for all reflections. The scan rate varied from 2.0 to $5.0^\circ/\text{min}$ depending inversely upon the intensity of the reflection. Stationary background counts were taken at lowest and highest 2θ values of the individual reflections for 0.4 times the scan time for $2.0^\circ \leq 2\theta \leq 45^\circ$ and 0.5 times the scan time for $45^\circ < 2\theta \leq 55^\circ$. Three standard reflections were measured between every 97 reflections and showed an approximately linear decay with time. After 139 h of data collection, the average standard intensity had dropped by 39%. Decay factors were applied in a stepwise manner. A total of 5595 reflections were scanned, resulting in 3201 unique observed ($I \geq 2\sigma(I)$) reflections.

Gaussian absorption corrections¹² were applied ($\mu = 10.61$ cm⁻¹) and the transmission coefficients ranged from 1.39 to 1.48.

A Patterson map indicated the position of the copper atom, which refined¹³ to a conventional R value¹⁴ of $R_1 = 40\%$ with use of unit weights. The corresponding Fourier synthesis showed the locations of all other nonhydrogen atoms. Hydrogen atoms were placed on the

Table II. Interatomic Distances^a (Å)

Cu-Cu'	3.0351 (9)	C(31)-C(32)	1.391 (4)
Cu-O(1)	1.962 (2)	C(31)-C(36)	1.385 (4)
Cu-O(1')	1.931 (2)	C(32)-C(33)	1.379 (5)
Cu-O(2)	1.890 (2)	C(33)-C(34)	1.382 (5)
Cu-O(3)	1.908 (2)	C(34)-C(35)	1.384 (5)
Cu-N(1)	2.298 (3)	C(34)-O(37)	1.350 (4)
O(1)-C(1)	1.324 (4)	C(35)-C(36)	1.375 (5)
O(2)-C(3)	1.300 (3)	O(37)-C(38)	1.424 (5)
O(3)-C(4)	1.280 (4)	C(41)-C(42)	1.402 (4)
C(1)-C(5)'	1.399 (4)	C(41)-C(46)	1.391 (4)
C(1)-C(2)	1.417 (4)	C(42)-C(43)	1.383 (5)
C(2)-C(3)	1.378 (4)	C(43)-C(44)	1.389 (5)
C(3)-C(31)	1.488 (4)	C(44)-C(45)	1.385 (5)
C(4)-C(5)	1.396 (4)	C(44)-O(47)	1.360 (4)
C(4)-C(41)	1.484 (4)	C(45)-C(46)	1.385 (5)
N(1)-C(91)	1.338 (5)	O(47)-C(48)	1.427 (6)
N(1)-C(95)	1.339 (5)		
C(91)-C(92)	1.371 (6)		
C(92)-C(93)	1.360 (7)		
C(93)-C(94)	1.376 (7)		
C(94)-C(95)	1.367 (6)		

^a All primed atoms have the \bar{x} , \bar{y} , \bar{z} symmetry transformed coordinates.

Table III. Interatomic Angles^a (Deg)

N(1)-Cu-O(1)'	96.00 (9)	C(36)-C(31)-C(32)	116.6 (3)
N(1)-Cu-O(1)	93.56 (9)	C(36)-C(31)-C(3)	119.8 (3)
N(1)-Cu-O(2)	92.24 (9)	C(32)-C(31)-C(3)	123.6 (3)
N(1)-Cu-O(3)	105.76 (9)	C(33)-C(32)-C(31)	121.3 (3)
O(1)-Cu-O(1)'	77.56 (9)	C(32)-C(33)-C(34)	120.9 (3)
O(1)-Cu-O(2)	91.70 (8)	C(37)-C(34)-C(33)	116.0 (3)
O(1)-Cu-O(3)	159.44 (11)	O(37)-C(34)-C(35)	125.3 (3)
O(1)'-Cu-O(2)	166.81 (9)	C(33)-C(34)-C(35)	118.7 (3)
O(1)'-Cu-O(3)	93.22 (8)	C(36)-C(35)-C(34)	119.6 (3)
O(2)-Cu-O(3)	94.43 (9)	C(35)-C(36)-C(31)	122.9 (3)
Cu-O(1)-Cu'	102.44 (9)	C(34)-O(37)-C(38)	117.6 (3)
C(1)-O(1)-Cu'	128.4 (2)	C(46)-C(41)-C(42)	116.8 (3)
C(1)-O(1)-Cu	125.7 (2)	C(46)-C(41)-C(4)	123.7 (3)
C(3)-O(2)-Cu	124.9 (2)	C(42)-C(41)-C(4)	119.4 (3)
C(4)-O(3)-Cu	126.0 (2)	C(43)-C(42)-C(41)	121.7 (3)
C(91)-N(1)-Cu	121.2 (2)	C(42)-C(43)-C(44)	120.1 (3)
C(95)-N(1)-Cu	121.6 (2)	O(47)-C(44)-C(45)	124.5 (3)
O(1)-C(1)-C(5)	119.5 (3)	O(47)-C(44)-C(43)	116.2 (3)
O(1)-C(1)-C(2)	119.2 (3)	C(45)-C(44)-C(43)	119.3 (3)
C(5)-C(1)-C(2)	121.3 (3)	C(44)-C(45)-C(46)	120.0 (3)
C(3)-C(2)-C(1)	126.7 (3)	C(45)-C(46)-C(41)	122.1 (3)
O(2)-C(3)-C(2)	125.7 (3)	C(44)-O(47)-C(48)	117.1 (3)
O(2)-C(3)-C(31)	113.7 (2)	C(91)-N(1)-C(95)	117.1 (3)
C(2)-C(3)-C(31)	120.6 (3)	N(1)-C(91)-C(92)	123.2 (4)
O(3)-C(4)-C(5)	124.8 (3)	C(93)-C(92)-C(91)	118.7 (4)
O(3)-C(4)-C(41)	115.4 (3)	C(92)-C(93)-C(94)	119.2 (4)
C(5)-C(4)-C(41)	119.8 (3)	C(95)-C(94)-C(93)	118.8 (5)
C(4)-C(5)-C(1)'	128.0 (3)	N(1)-C(95)-C(94)	122.9 (4)

^a All primed atoms have \bar{x} , \bar{y} , \bar{z} symmetry transformed coordinates.

basis of peaks in a difference Fourier calculation and were assigned isotropic temperature factors equal to those of the carbon atom to which they were bound. Hydrogen temperature parameters were held invariant throughout the refinement. Full-matrix least-squares calculations, using our usual weighting scheme,¹⁵ of all positional and anisotropic temperature parameters reached convergence at $R_1 = 0.035$ and $R_2 = 0.050$.¹⁴ On the last cycle, the number of variables was 343, the maximum shift/error was 0.3σ and the error in an observation of unit weight was 1.475. The highest peak on a difference Fourier map represented 0.3 electron and was located 0.8 Å from O(3).

Neutral-atom scattering factors¹⁶ were used including anomalous dispersion¹⁷ for Cu. An examination of the error of fit over intervals

(11) "International Tables for X-ray Crystallography", 3rd ed.; Kynoch Press: Birmingham, England, 1969; Vol. 1.

(12) The mga computing programs were local modifications of ABSORB, Zalkin's FORDAP, Johnson's ORTEP, and Busing-Martin-Levy's ORFLS and ORFEE.

(13) The function minimized was $\sum w(|F_o| - |F_c|)^2$.

(14) $R_1 = \sum ||F_o| - |F_c|| / \sum |F_o|$; $R_2 = [\sum w(|F_o| - |F_c|)^2]^{1/2} / [\sum w F_o^2]^{1/2}$.

(15) $w = F^2 / \sigma(F^2)^2$.

(16) (a) Cromer, D. T.; Mann, J. B. *Acta Crystallogr., Sect. A* **1968**, *A24*, 321. (b) Stewart, R. F.; Davidson, E. R.; Simpson, W. T. *J. Chem. Phys.* **1965**, *42*, 3175.

Table IV. Anisotropic Thermal Parameter^a

atom	β_{11}	β_{22}	β_{33}	β_{12}	β_{13}	β_{23}
Cu	0.01119 (6)	0.00115 (1)	0.00547 (3)	-0.00023 (2)	0.00139 (3)	0.00002 (1)
O(1)	0.01354 (36)	0.00115 (4)	0.00554 (17)	-0.00028 (9)	0.00185 (20)	-0.00006 (6)
O(2)	0.01341 (35)	0.00111 (4)	0.00677 (18)	-0.00038 (10)	0.00311 (20)	-0.00012 (7)
O(3)	0.01582 (39)	0.00118 (4)	0.00602 (17)	-0.00058 (10)	0.00218 (21)	0.00007 (7)
C(1)	0.01016 (46)	0.00128 (6)	0.00611 (25)	-0.00002 (13)	0.00054 (28)	0.00007 (10)
C(2)	0.01559 (58)	0.00112 (6)	0.00650 (29)	-0.00043 (15)	0.00285 (32)	-0.00034 (10)
C(3)	0.00896 (44)	0.00147 (6)	0.00618 (25)	0.00002 (14)	0.00077 (26)	-0.00009 (10)
C(4)	0.00975 (47)	0.00135 (6)	0.00576 (25)	-0.00005 (13)	0.00070 (27)	0.00039 (10)
C(5)	0.01652 (60)	0.00116 (6)	0.00678 (28)	-0.00053 (16)	0.00292 (33)	-0.00014 (10)
C(31)	0.01137 (49)	0.00128 (6)	0.00596 (25)	-0.00021 (13)	0.00069 (28)	-0.00011 (9)
C(32)	0.02263 (77)	0.00142 (7)	0.00684 (30)	0.00037 (18)	0.00382 (38)	0.00026 (11)
C(33)	0.02602 (87)	0.00128 (7)	0.00798 (33)	0.00062 (20)	0.00443 (42)	0.00002 (12)
C(34)	0.01525 (59)	0.00163 (7)	0.00609 (27)	-0.00046 (16)	0.00102 (31)	-0.00032 (10)
C(35)	0.02257 (76)	0.00164 (7)	0.00553 (28)	0.00002 (19)	0.00188 (36)	0.00040 (11)
C(36)	0.02021 (70)	0.00116 (6)	0.00700 (29)	-0.00004 (17)	0.00138 (35)	0.00003 (11)
O(37)	0.02631 (57)	0.00180 (5)	0.00639 (20)	-0.00044 (14)	0.00407 (27)	-0.00055 (8)
C(38)	0.02172 (85)	0.00254 (10)	0.00579 (31)	0.00015 (23)	0.00196 (40)	-0.00034 (13)
C(41)	0.01141 (49)	0.00140 (6)	0.00570 (25)	-0.00013 (14)	0.00078 (28)	0.00028 (9)
C(42)	0.01826 (65)	0.00146 (7)	0.00645 (27)	-0.00064 (17)	0.00160 (33)	0.00002 (11)
C(43)	0.01934 (69)	0.00190 (8)	0.00638 (29)	-0.00034 (19)	0.00347 (36)	0.00036 (12)
C(44)	0.01470 (60)	0.00170 (7)	0.00629 (27)	-0.00063 (16)	0.00180 (32)	0.00069 (11)
C(45)	0.01928 (71)	0.00141 (7)	0.00850 (34)	-0.00117 (18)	0.00163 (39)	0.00006 (12)
C(46)	0.01865 (67)	0.00156 (7)	0.00636 (29)	-0.00053 (17)	0.00347 (36)	-0.00002 (11)
O(47)	0.02200 (51)	0.00202 (6)	0.00822 (23)	-0.00171 (14)	0.00402 (28)	0.00079 (9)
C(48)	0.02949 (**)	0.00232 (12)	0.01365 (55)	-0.00361 (30)	0.00541 (68)	0.00114 (20)
N(1)	0.01136 (44)	0.00187 (7)	0.00813 (25)	0.00009 (13)	0.00002 (27)	0.00027 (10)
C(91)	0.01317 (63)	0.00262 (10)	0.00985 (38)	0.00037 (19)	0.00101 (39)	0.00056 (15)
C(92)	0.01122 (68)	0.00422 (16)	0.01496 (61)	0.00040 (24)	0.00353 (49)	0.00132 (24)
C(93)	0.01151 (69)	0.00471 (17)	0.01634 (66)	-0.00217 (29)	-0.00349 (54)	0.00257 (27)
C(94)	0.01839 (83)	0.00337 (12)	0.01123 (48)	-0.00161 (26)	-0.00444 (52)	0.00052 (19)
C(95)	0.01474 (66)	0.00247 (9)	0.00868 (36)	-0.00007 (19)	-0.00142 (39)	0.00035 (14)

^a The form of the anisotropic thermal ellipsoid is $\exp[-(\beta_{11}h^2 + \beta_{22}k^2 + \beta_{33}l^2 + 2\beta_{12}hk + 2\beta_{13}hl + 2\beta_{23}kl)]$.

Table V. Hydrogen Positional and Isotropic Thermal Parameters^{a,b}

atom	x	y	z	B, Å ²
H(2)	0.015 (3)	-0.172 (1)	-0.164 (3)	3.05
H(5)	0.075 (4)	0.181 (1)	-0.033 (3)	3.25
H(32)	0.126 (4)	-0.210 (1)	-0.299 (3)	4.04
H(33)	0.207 (4)	-0.251 (2)	-0.492 (3)	4.20
H(35)	0.202 (4)	-0.097 (1)	-0.637 (3)	3.99
H(36)	0.130 (4)	-0.056 (2)	-0.461 (3)	3.70
H(38a)	0.237 (4)	-0.150 (2)	-0.810 (3)	4.56
H(38b)	0.391 (4)	-0.143 (2)	-0.742 (3)	4.56
H(38c)	0.353 (4)	-0.201 (2)	-0.821 (3)	4.56
H(42)	0.239 (4)	0.116 (1)	-0.387 (3)	3.50
H(43)	0.394 (4)	0.184 (1)	-0.496 (3)	3.85
H(45)	0.320 (4)	0.311 (2)	-0.242 (3)	4.05
H(46)	0.184 (4)	0.243 (1)	-0.136 (3)	3.75
H(48a)	0.589 (5)	0.337 (2)	-0.344 (4)	5.72
H(48b)	0.437 (5)	0.365 (2)	-0.436 (4)	5.72
H(48c)	0.579 (5)	0.359 (2)	-0.474 (3)	5.72
H(91)	-0.317 (4)	0.040 (2)	-0.059 (3)	4.51
H(92)	-0.565 (5)	0.038 (2)	-0.130 (4)	5.77
H(93)	-0.630 (5)	-0.014 (2)	-0.323 (4)	6.38
H(94)	-0.435 (5)	-0.051 (2)	-0.420 (4)	6.12
H(95)	-0.182 (4)	-0.046 (2)	-0.355 (3)	4.64

^a Isotropic thermal parameters for hydrogen atoms were assigned to be equivalent to the isotropic parameter of the carbon atom to which it is bound and were held invariant. ^b H(n) is bound to C(n).

of increasing F_o and $(\sin \theta)/\lambda$ showed only minor deviations. The value of p in the calculation of $\sigma(I)$ was 0.05. Final atomic positional parameters are presented in Table I. Interatomic distances and bond angles are listed in Tables II and III respectively. Tables containing anisotropic thermal parameters, hydrogen bond lengths and angles, hydrogen positional and isotropic parameters, RMS displacements, and calculated and observed F_o 's are available as supplementary material.

Table VI. Least-Squares Planes

Plane Deviations, Å			
atom ^b	I	II	III
Cu	-0.237	-0.458	0.026
O(1)	0.088*	0.024*	
O(2)	-0.077*	-0.025*	
O(3)	0.076*		-0.005
O(1)'	-0.087*		0.000*
C(1)		-0.026*	
C(2)		-0.002*	
C(3)		0.029*	
C(4)			0.011*
C(5)			-0.011*
C(1)'			0.005*

Equation of the Plane: $ax + by + cz = d^c$

plane	a	b	c	d
I	-0.9337	0.0015	-0.3580	0.0004
II	-0.9393	0.1636	-0.3014	-0.2671
III	-0.9074	0.2078	-0.3654	0.3309

^a The atoms that define the plane are marked with an asterisk. The estimated errors are about 0.008 Å. ^b All primed atoms have the \bar{x} , \bar{y} , \bar{z} symmetry transformed coordinates. ^c Where x , y , and z are fractional cell edges.

Results

The structure of Cu₂DANA₂(py)₂ consists of discrete binuclear units in which each copper atom is five-coordinate in an approximate square-pyramidal arrangement. No atoms are located within 3.5 Å of the vacant sixth position of the copper atoms, and intermolecular copper atoms are separated by at least 8.19 Å, so that clearly any magnetic coupling must arise from intramolecular interactions.

Crystallographic symmetry requires an inversion center in the molecule, with the result that the bridged copper atoms are in identical environments. The triketonate, DANA²⁻, ligands are planar (see Table VI, planes II and III) with a

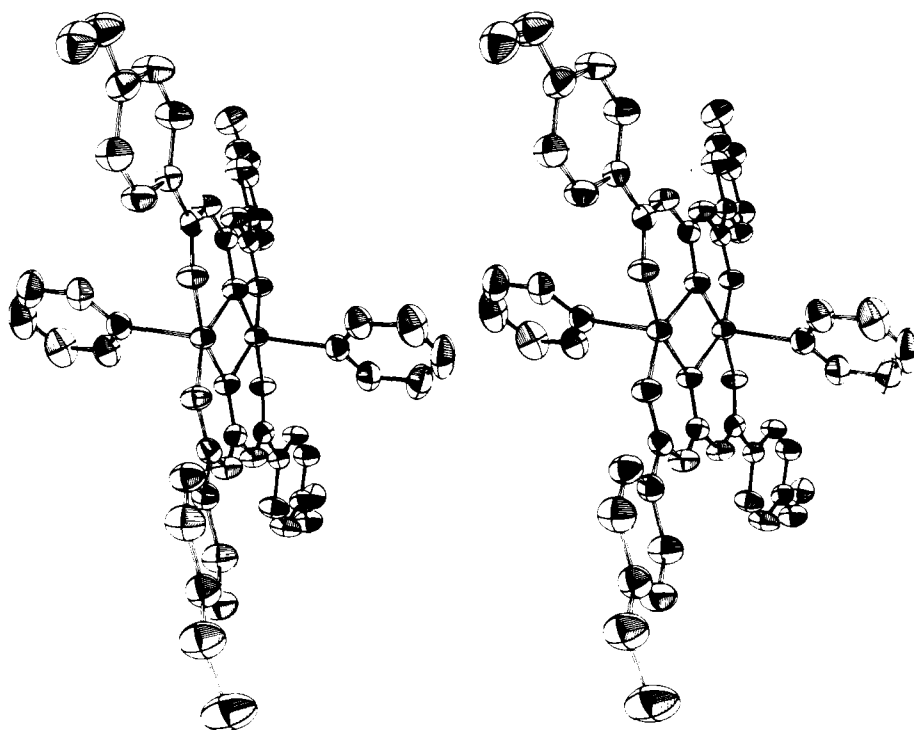


Figure 1.

Table VII. Bond Lengths Involving Hydrogen (Å)

C(2)-H(2)	0.95 (3)	C(45)-H(45)	0.98 (3)
C(5)-H(5)	0.83 (3)	C(46)-H(46)	0.90 (3)
C(32)-H(32)	0.98 (3)	C(48)-H(48a)	0.75 (4)
C(33)-H(33)	0.89 (4)	C(48)-H(48b)	1.01 (4)
C(35)-H(35)	0.89 (3)	C(48)-H(48c)	1.08 (4)
C(36)-H(36)	0.92 (3)	C(91)-H(91)	1.01 (4)
C(38)-H(38a)	0.85 (4)	C(92)-H(92)	0.87 (4)
C(38)-H(38b)	0.97 (4)	C(93)-H(93)	0.89 (4)
C(38)-H(38c)	0.98 (4)	C(94)-H(94)	0.91 (4)
C(42)-H(42)	1.03 (3)	C(95)-H(95)	1.00 (4)
C(43)-H(43)	0.97 (3)		

Table VIII. Bond Angles (Deg) Involving Hydrogen

H(2)-C(2)-C(3)	117 (2)	H(42)-C(42)-C(43)	117 (2)
H(2)-C(2)-C(1)	116 (2)	H(42)-C(42)-C(41)	122 (2)
H(5)-C(5)-C(4)	117 (2)	H(43)-C(43)-C(42)	123 (2)
H(5)-C(5)-C(1')	115 (2)	H(43)-C(43)-C(44)	116 (2)
H(32)-C(32)-C(33)	125 (2)	H(45)-C(45)-C(44)	125 (2)
H(32)-C(32)-C(31)	113 (2)	H(45)-C(45)-C(46)	115 (2)
H(33)-C(33)-C(32)	125 (2)	H(46)-C(46)-C(45)	122 (2)
H(33)-C(33)-C(34)	114 (2)	H(46)-C(46)-C(41)	116 (2)
H(35)-C(35)-C(36)	120 (2)	H(48a)-C(48)-H(48b)	143 (5)
H(35)-C(35)-C(34)	120 (2)	H(48a)-C(48)-H(48c)	94 (3)
H(36)-C(36)-C(35)	119 (2)	H(48a)-C(48)-O(47)	107 (2)
H(36)-C(36)-C(31)	118 (2)	H(48b)-C(48)-H(48c)	93 (4)
H(38a)-C(38)-H(38c)	114 (3)	H(48b)-C(48)-O(47)	106 (4)
H(38a)-C(38)-H(38b)	99 (3)	H(48c)-C(48)-O(47)	105 (2)
H(38a)-C(38)-O(37)	108 (2)	H(91)-C(91)-N(1)	115 (2)
H(38b)-C(38)-H(38c)	125 (3)	H(91)-C(91)-C(92)	121 (2)
H(38b)-C(38)-O(37)	110 (2)	H(92)-C(92)-C(93)	130 (3)
H(38c)-C(38)-O(37)	100 (3)	H(92)-C(92)-C(91)	111 (3)
		H(93)-C(93)-C(92)	131 (3)
		H(93)-C(93)-C(94)	110 (3)
		H(94)-C(94)-C(95)	119 (3)
		H(94)-C(94)-C(93)	122 (3)
		H(95)-C(95)-N(1)	123 (2)
		H(95)-C(95)-C(94)	114 (2)

dihedral angle of 4.8° between them. Each copper atom is bound to two terminal ketonate oxygen atoms and two bridging ketonate oxygen atoms. The fifth positions are occupied by σ -bonded pyridine molecules which are located on either side of the (DANA)₂ plane (see Figure 1). In typical five-coor-

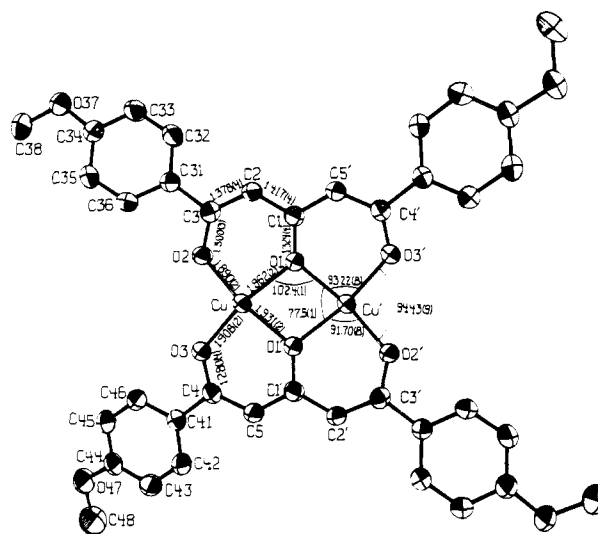


Figure 2.

dinate fashion, copper lies 0.24 \AA above the donor oxygen plane toward the nitrogen atom of pyridine. Figure 2 shows the $\text{Cu}_2(\text{DANA})_2(\text{py})_2$ molecule with the axial pyridine ligands removed for clarity and illustrates the numbering scheme, selected bond lengths, and selected bond angles. A packing diagram as viewed down the a axis is available as supplementary material. Figure 3 presents a view of the molecule that shows the orientation of the pyridine ligands with respect to the Cu-O bonds.

The results of the temperature-dependent magnetic susceptibility measurements for $(\text{VO})_2(\text{DANA})_2$ are shown in Figure 4. The antiferromagnetism is apparent from the decreasing magnetic moment with decreasing temperatures and from the well-defined transition temperature at 125 K. The exchange constant, J , calculated with use of the Bleaney-Bowers¹⁸ equation is equal to -80 cm^{-1} . The results of this treatment showing the "fit" between calculated and measured

Table IX. Calculated and Observed Magnetic Susceptibility as a Function of Temperature for $(\text{VO})_2(\text{DANA})_2$

T, K	$10^6 \times (\chi_m - N\alpha)_{\text{obsd.}}$ cgsu	$10^6 \times (\chi_m - N\alpha)_{\text{calcd.}}^a$ cgsu	% diff
350	910	840	-7.7
333	930	871	-6.4
298	950	941	-1.0
273	990	1000	+1.0
173	1160	1230	+5.7
143	1130	1255	+10.0
123	1150	1226	+6.2
77	1010	800	-20

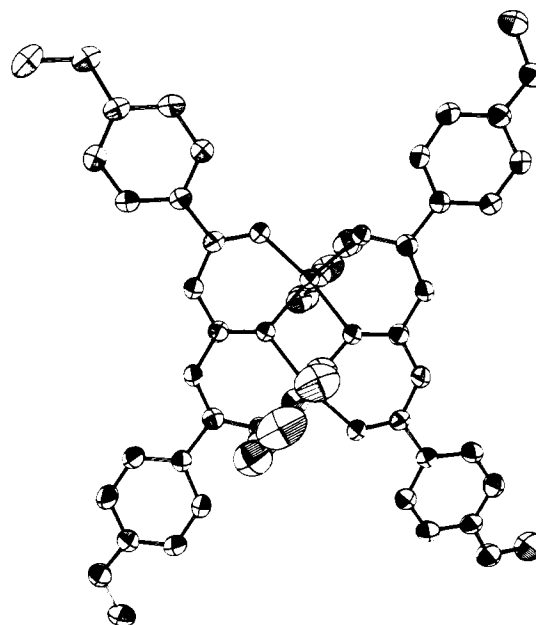
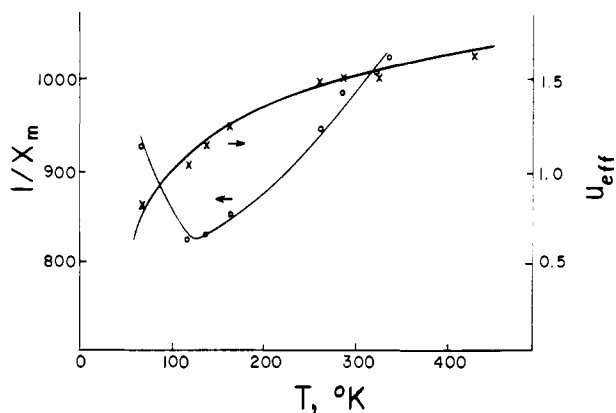
^a Calculated with use of the Bleaney-Bowers equation with $g = 1.97$, $2J = -160 \text{ cm}^{-1}$, and $N\alpha = 60 \times 10^{-6}$.

susceptibilities are shown in Table IX. The g value used in the calculation is 1.97 which is the g_{av} measured from the EPR spectrum obtained in pyridine.

The magnetic susceptibility of $\text{Cu}_2(\text{DANA})_2(\text{py})_2$ is extremely low even at room temperature. The measured value of $\chi_m' - N\alpha$ at 300 K is 125×10^{-6} cgsu per Cu. At 77 K the measured $\chi_m' - N\alpha$ is 100×10^{-6} cgsu. The very small weight changes observed experimentally mean a relatively large uncertainty in these values. The estimated error based on several measurements is about $\pm 20 \times 10^{-6}$. The susceptibility measured at 77 K is attributed to a small amount of mononuclear Cu(II) impurity since the 300 K value predicts that the susceptibility would be zero at temperatures much above 77 K. On this basis the experimental values were corrected for 2% mononuclear impurity. The corrected value of $(\chi_m' - N\alpha)_{\text{obsd}}$ at 300 K is $100 (\pm 20) \times 10^{-6}$ cgsu per Cu. This value may be calculated with use of the Bleaney-Bowers¹⁸ equation with $2J = -825 (\pm 50) \text{ cm}^{-1}$, $g = 2.10$, and $N\alpha = 75 \times 10^{-6}$.

Discussion

The structures of a number of binuclear complexes containing 1,3,5-triketone ligands or their diamine Schiff-base derivatives have been determined, thereby providing a basis for comparison of various metal ion coordination spheres. These structures include heterobinuclear^{1,2} and homobinuclear³⁻⁸ complexes with $M = \text{V},^{1,2} \text{Zn},^2 \text{Co},^3 \text{Ni},^{2,4,5,8}$ and $\text{Cu}.$ ⁶⁻⁸ The salient features of such comparisons are generally those that influence the magnetic exchange, i.e., the M-M distance, the M-O_b-M angle, the O_b-M-O_b angle, and the deviation of M from the ligand plane. The complexes that have been structurally characterized can be loosely grouped into two classes: (1) those with six-coordinate metal ions and (2) those with five-coordinate metal ions. The cobalt(II)³ and nickel(II)^{4,5,8} triketonates with pyridines occupying the 5th and 6th

**Figure 3.****Figure 4.**

coordination sites belong to the first class. In these compounds the Co and Ni atoms are in the plane of the triketone moieties. The binuclear Cu(II) complexes⁶⁻⁸ and the heterobinuclear complexes containing VO^{2+2} and $\text{Zn}(\text{II})^2$ belong to the second class. In these compounds the metal atoms are somewhat out of the plane of the ligands in typical five-coordinate fashion. These structural results are summarized in Table X and XI for several homobinuclear complexes, two

Table X. Summary of Structural Data Pertinent to Magnetic Exchange in Homobinuclear Triketonates

compd	coord no.	dist, Å					angles, deg		ref
		M-M	M-B ^a	M out of plane	M-O _b	M-O _t	O _b -M-O _b	M-O _b -M	
$\text{Cu}_2(\text{DANA})_2(\text{py})_2$	5	3.035 (1)	2.298 (3)	0.237	1.962 (2), 1.931 (2)	1.890 (2), 1.908 (2)	77.56 (9)	102.44 (9)	this work
$\text{Cu}_2(\text{BAA})_2(\text{py})_2$	5	3.055 (3)	2.274 (10)	0.23	1.942 (11), 1.948 (11)	1.914 (10), 1.901 (11)	76.6	103.5	6
$\text{Cu}_2(\text{DAA})_2(\text{py})_2$	5	3.051 (3)	2.32	0.28	1.97, 1.92	1.94, 1.88	77	103	7
$\text{Cu}_2(\text{HXFDAA})_2(\text{CH}_3\text{OH})_2$	5	3.040 (3)	2.223 (11)	0.21	1.938 (4)	1.901 (6)	76.7 (3)	103.3 (3)	8
$[\text{Cu}_2(\text{DTFACP})_2\text{H}_2\text{O}]_2$	6	3.064 (8)	2.307 (7)	0.10	1.925 (6), 3.068 (7)	1.896 (7), 1.904 (7)	75.1 (2)	103.8	6
$\text{Co}_2(\text{DBA})_2(\text{py})_4$	6	3.272 (3)	2.200 (10)	0.0	2.097 (7), 2.091 (7)	2.012 (7), 2.005 (7)	77.3	102.7	3
$\text{Ni}_2(\text{DBA})_2(\text{py})_4$	6	3.166 (3)	2.155 (8)	0.01	2.046 (6), 2.042 (6)	2.013 (6), 2.014 (6)	78.5	101.5	4
$\text{Ni}_2(\text{TFDAA})_2(\text{py})_4$	6	3.161 (3)	2.136 (9)	0.01	2.046 (6), 2.046 (6)	2.018 (7), 2.015 (7)	78.9 (2)	101.1 (2)	8

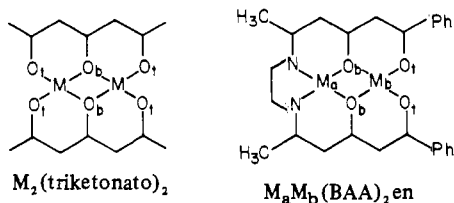
^a B is the neutral, adduct ligand donor atom.

Table XI. Summary of Structural Data for Heterobinuclear and Mononuclear Complexes $M_a-M_b(BAA)_2en$ and $M_bH_2(BAA)_2en^a$

compd	M_a	M_b	coord		dist, Å					angles, deg			ref
			no. M_b	M_a-M_b	M_b-B	M_b out of plane	M_a-O_b	M_b-O_b	M_b-O_t	$O_b-M_a-O_b$	$O_b-M_b-O_b$	$M_a-O_b-M_b$	
NiVO(BAA) ₂ en	Ni	VO	5	2.991	1.591	0.616	1.854, 1.847	1.979, 1.990	1.912, 1.919	78.9	72.7	102.5	2
NiZn(py)(BAA) ₂ en	Ni	Zn(py)	5	3.120	2.088	0.382	1.841, 1.850	2.102, 2.081	1.948, 1.949	79.8	69.0	104.4	2
NiNi(py) ₂ (BAA) ₂ en	Ni	Ni(py) ₂	6	3.04	2.12	0.02	1.855, 1.858	2.030, 2.047	1.993, 2.002	81.7	73.1	102.6	5
VOH ₂ (BAA) ₂ en ^b		VO	5		1.625	0.564		1.964, 1.961	1.923, 1.936		81.9		1
[CuH ₂ (BAA) ₂ en] ₂ ^b		Cu	5		2.603 ^c	0.06		1.916, 1.903	1.902, 1.895		85.1		6

^a H₂(BAA)₂en is the ligand resulting from the condensation of 1-phenyl-1,3,5-hexanetrione and ethylenediamine. ^b The single metal ion is coordinated to the four ketonic oxygens. ^c The ketonic oxygen from an adjacent molecule is the fifth ligand thus forming a dimeric unit.

heterobinuclear complexes, one mixed-spin-state binuclear complex and two mononuclear complexes. The generalized structures (omitting adduct ligands) with the labels used in Table X and XI are



The bridging angle, $M-O_b-M$, which is generally thought to be important in determining the sign and magnitude of the magnetic exchange is relatively constant throughout the entire series. The average for the 11 molecules in Tables X and XI is 102.8° with a maximum deviation of $\pm 1.7^\circ$ or about 1.6%. Of the homobinuclear triketonates in Table X the trend in the metal-metal distance is $Co (3.27 \text{ \AA}) > Ni (3.16 \text{ \AA}) > Cu (3.05 \text{ \AA})$ which parallels to the trend in the size of the equivalent ions. For any given metal ion the $M-M$ distance is quite constant. The observed trend in $M-M$ distance is reflected in the $M-O_b$ bond distances which average 2.09 \AA for Co, 2.04 \AA for Ni, and 1.95 \AA for Cu. The tendency for $M-O_b$ to be longer than $M-O_t$ is constant throughout the entire series. It does not appear that the explanation of this result lies solely in the fact that the bridging oxygen has two metals coordinated to it and the terminal oxygens only one since, even in the mononuclear complex $VOH_2(BAA)_2en$, $M-O_b > M-O_t$ and both oxygens are bonded to only one metal atom. In addition, this tendency for a lengthened $M-O_b$ bond is not present in either the structure of N,N' -ethylene(salicylideneiminato)copper(II)-bis(hexafluoroacetylacetonato)cobalt(II) reported by Drago et al.¹⁹ or $[Cu(PIA)]_2$ reported by Bertrand and Kelley.²⁰ Therefore, the trend for $M-O_b > M-O_t$ in the triketonate-type complexes must in part be due to electronic effects in the ligands and not simply a consequence of bridging. This is supported by the fact that in the complexes the central carbonyl bond distance is typically about 0.03 \AA longer than the terminal carbonyls, 1.32 v. 1.29 \AA .

Several of the binuclear molecules whose structures have been determined contain pyridine as the adduct ligand occupying the fifth or the fifth and sixth coordination positions. Examples with pyridine coordinated to Co, Ni, Cu, and Zn are available. In the three binuclear copper complexes containing pyridines as the fifth ligand on the coppers, in each case the plane of the pyridine is coincident with one set of

O_b-Cu-O_t bond (see Figure 3). However, in all cases in which Co, Ni, or Zn is bonded to one or two pyridines, the plane of the pyridine bisects an $O-Cu-O$ angle. It might be argued that in $Co_2(DBA)_2(py)_4$, $Ni_2(DBA)_2(py)_4$, and $Ni_2(TFDA)_2(py)_4$ this arrangement of the pyridines (parallel and bisecting O_t-M-O_b angles) is due to steric considerations. This is not the case in $NiZn(py)(BAA)_2en$ or $NiNi(py)_2(BAA)_2en$, however. Interestingly, in $NiNi(py)_2(BAA)_2en$ the two pyridines on the high-spin Ni(II) have planes that are perpendicular to one another and bisect different $O-Cu-O$ angles. Thus, there appears to be a bonding interaction between the Ni and the pyridines similar to that discussed by Elder²¹ in which he postulated that such an arrangement permits maximum π bonding between the metal and the pyridine. There is no apparent steric or crystal packing explanation for different arrangement of the pyridines in the copper compounds, and so one suspects that there is an additional (or different) interaction present in these compounds.

Although the structure of $(VO)_2(DANA)_2$ has not been determined (nor any other binuclear vanadyl triketonate), the available structural data allow one to make very reasonable estimates of those structural parameters of interest to the magnetic properties. For example, $NiVO(BAA)_2N$, $VOH_2(BAA)_2en$, $VO(1\text{-phenyl-1,3-butanedionato})_2$ ²² results predict that the V atom is about 0.58 \AA out of the ligand plane and, based on the copper complexes, it is reasonable to expect one V atom above and one below the ligand plane. It also seems safe enough to predict a $V-O_b-V$ bridging angle of $103^\circ \pm 1.5^\circ$ and $V-V$ distance of $3.0-3.1 \text{ \AA}$. The point of making the predictions is, of course, to emphasize that these structural parameters are expected to be very similar in $Cu_2(DANA)_2(py)_2$ and $(VO)_2(DANA)_2$. It is likely that the most significant structural difference between them is that the coppers are 0.24 \AA out of plane while the vanadium atoms are about 0.58 \AA out of plane.

A comparison between the magnetic properties of these structurally similar d^1-d^1 and d^2-d^2 complexes illustrates very well the importance of the orbital symmetry of the unpaired electrons. In the binuclear copper(II) triketonates it seems clear that the odd electron on each copper has its origin in the atomic orbital that is directed toward the bridging oxygen. Thus, one can consider mechanisms such as three-centered molecular orbital formation or spin polarizations to explain the strong d^2-d^2 exchange. Whatever the details of the exchange mechanism, it is reasonable to assume that it operates through the σ -orbital system of the four-membered Cu_2O_2 ring. Although the ring in $Cu_2(DANA)_2(py)_2$ is not strictly planar (since the five-coordinate coppers are about 0.24 \AA out of the ligand plane) the exchange is almost strong enough to com-

(19) O'Brien, N. B.; Maier, T. O.; Paul, I. C.; Drago, R. S. *J. Am. Chem. Soc.* **1973**, *95*, 6640.

(20) Bertrand, J. A.; Kelley, J. A. *Inorg. Chim. Acta* **1970**, *4*, 203.

(21) Elder, R. C. *Inorg. Chem.* **1968**, *7*, 1117.

(22) Hon, P. K.; Belford, R. L.; Pfluger J. *Chem. Phys.* **1965**, *43*, 1323.

pletely spin pair the electrons. Similar results are obtained in other triketonates in which the copper atoms are 0.24 Å above and below the best plane.⁶⁻⁸ While it does seem reasonable to expect this nonplanarity to result in less efficient orbital overlap and, as a result, weaker magnetic exchange, the observed distortion is apparently a relatively small perturbation.

The electronic configuration in $(VO)_2(DANA)_2$ is somewhat less certain than in the analogous Cu(II) compound. However, it is certain that the unpaired electron on each VO^{2+} is not in a σ -symmetry orbital. Since the ground state of the homologous mononuclear 1,3-diketonates $VO(1,3\text{-diketonato})_2$ is considered to be d^{1}_{xy} ,²³ it is logical to believe that similar states are appropriate for each VO^{2+} in $(VO)_2(DANA)_2$. If the unpaired electrons are initially in d_{xy} orbitals, the possibility of a direct metal-metal interaction must be considered since d_{xy} is directed between the bridging oxygens. The distance between the vanadium is large (ca. 3.0-3.2 Å), and one would expect a weak exchange for the direct metal-metal interaction. Other superexchange mechanisms involving the bridging ox-

xygen and metal orbitals are less convincing since they involve electron excitation into orbitals of appropriate symmetry followed by exchange in these excited states.²⁴

Regardless of the details of the exchange mechanisms it is true that the strength of the exchange as measured by the exchange constant, J , is about five times as large for $Co_2(DANA)_2(py)_2$ as for $(VO)_2(DANA)_2$. In these structurally similar molecules it is reasonable to attribute most of the difference to the spatial orientation of the exchanging electrons.

Acknowledgment is made to the National Science Foundation, Grant CHE-77-02664, and to the donors of the Petroleum Research Fund, administered by the American Chemical Society, for support of this research.

Registry No. $(VO)_2(DANA)_2$, 75880-93-2; $Cu_2(DANA)_2$, 29745-69-5; $Cu_2(DANA)_2(py)_2$, 75880-94-3.

Supplementary Material Available: Listings of structure factor amplitudes and a packing diagram (18 pages). Ordering information is given on any current masthead page.

(23) C. J. Ballhausen and H. B. Gray *Inorg. Chem.* **1962**, *1*, 111.

(24) See, for example: Martin, R. L. "New Pathways in Inorganic Chemistry"; Ebsworth, E. A. V., Maddock, A. G., Sharpe, A. G., Eds.; Cambridge University Press: London, 1968; Chapter 9.

Contribution from the Institut de Recherches sur la Catalyse, 69626 Villeurbanne Cédex, France

Opening of the P-N Bond of Bicyclic Phosphoranes. X-ray Crystal and Molecular Structures of Four Rhodium(I) Complexes of Perhydro-1,3,6,2-dioxazaphosphocine Ligands¹

DANIEL BONDOUX, BERNARD F. MENTZEN,* and IGOR TKATCHENKO*

Received March 6, 1980

The structures of $cis\text{-}L^1Rh(CO)Cl$, $cis\text{-}L^2Rh(CO)Cl$, $[L^2_2Rh]Cl$, and $[L^2_2Rh]ClO_4$, where L^1 and L^2 are the perhydro-dioxazaphosphocine ligands $C_6H_5POCH_2CH_2N(H)CH_2CH_2O$ and $C_6H_5POCH_2C(CH_3)_2N(H)CH_2CH_2O$, have been determined by three-dimensional X-ray diffraction studies. These compounds crystallize respectively in the space groups $Pbca$ ($a = 7.031$ (1) Å, $b = 11.509$ (2) Å, $c = 33.400$ (9) Å, $Z = 8$), $P2_1/c$ ($a = 11.692$ (2) Å, $b = 15.447$ (4) Å, $c = 9.202$ (2) Å, $\beta = 110.68$ (2)°, $Z = 4$), $C2/c$ ($a = 17.855$ (3) Å, $b = 13.567$ (2) Å, $c = 11.743$ (2) Å, $\beta = 107.60$ (2)°, $Z = 4$), and $P\bar{1}$ ($a = 9.856$ (3) Å, $b = 12.191$ (5) Å, $c = 12.469$ (3) Å, $\alpha = 71.58$ (3)°, $\beta = 85.00$ (3)°, $\gamma = 77.69$ (3)°, $Z = 2$). Diffraction data to respectively $2\theta_{max} = 60, 60, 72, \text{ and } 72^\circ$ (Mo $K\alpha$ radiation) were collected on an Enraf-Nonius CAD-4 fully automated four-circle diffractometer. The structures were solved by the heavy-atom method and refined by full-matrix least-squares procedures to conventional discrepancy indexes, respectively $R = 0.0308$ (1860 unique data), 0.0223 (2340), 0.0348 (2768), and 0.0586 (1464). For each case the configuration around Rh is square planar. The ligands L are in all cases of the bidentate P,N nature, with P...N distances in the range 2.788-2.853 Å, suggesting the lack of any dative P←N bond. The conformation of these ligands are of the chair-boat type with stronger deformations for the *gem*-dimethyl L^2 ligand. Some further deformations are indicated by the values observed for the Rh-P-C angles (ca. 125-130°) which deviate significantly from those reported for analogous phosphonites (ca. 118°). The complex $[L^2_2Rh]Cl$ presents a twofold axis which is in accordance with the occurrence of only one racemate in the crystal analyzed. In the complex $[L^2_2Rh]ClO_4$, only one oxygen atom of the perchlorate anion is asymmetrically bonded to the (N) hydrogens.

Introduction

The bicyclic phosphoranes **1** have attracted interest in the recent years owing to the possibility of equilibria with the tautomeric monocyclic structures **2-4** (Scheme I) containing now a P(III) site. Only compounds **1** are detected in solution² but, recently, the occurrence of form **2** has been evidenced in the gas phase by UPS.³ Nevertheless, a reaction occurs with

different transition-metal compounds leading to complexes where the monocyclic P,N form **2** is trapped and stabilized.^{4,5}

For the rhodium(I) complexes, bidentate ligation is obtained and P(III) coordination is involved since $^1J_{Rh-P}$ coupling is observed. However, neither NMR nor IR spectroscopy

(1) Paper 3 of this series. For papers 1 and 2, see ref 4 and 5.
 (2) Houalla, D.; Brazier, J.-F.; Sanchez, M.; Wolf, R. *Tetrahedron Lett.* **1972**, 2969. Houalla, D.; Mouheich, T.; Sanchez, M.; Wolf, R. *Phosphorus* **1975**, *5*, 229.

(3) Houalla, D.; Sanchez, M.; Goubeau, D.; Pfister-Guillouzo, G. *Nouv. J. Chim.* **1979**, *3*, 509.
 (4) Bondoux, D.; Tkatchenko, I.; Houalla, D.; Wolf, R.; Pradat, C.; Riess, J.; Mentzen, B. F. *J. Chem. Soc., Chem. Commun.* **1978**, 1022.
 (5) Pradat, C.; Riess, J. G.; Bondoux, D.; Mentzen, B. F.; Tkatchenko, I.; Houalla, D. *J. Am. Chem. Soc.* **1979**, *101*, 2234.